Towards electrical spin injection into LaAlO3-SrTiO3

M. Bibes, N. Reyren, E. Lesne, J.-M T George, C. Deranlot, S. Collin, A. Barthélémy, H. Jaffres

Towards electrical spin injection into $LaAlO_3/SrTiO_3$

M. Bibes, N. Reyren, E. Lesne, J.-M. George, C. Deranlot, S. Collin, A. Barthélémy, H.Jaffrès

Unité Mixte de Physique CNRS-Thales, 1 Av. A. Fresnel, 91767 Palaiseau, France,
and Université Paris-Sud, 91405 Orsay, France

Future spintronics devices will be built from elemental blocks allowing the electrical injection, propagation, manipulation and detection of spin-based information. Owing to their remarkable multifunctional and strongly correlated character, oxide materials already provide such building blocks for charge-based devices such as ferroelectric field-effect transistors, as well as for spin-based two-terminal devices like magnetic tunnel junctions, with giant responses in both cases. Until now, the lack of suitable channel materials and the uncertainty of spin injection conditions in these compounds had however prevented the exploration of similar giant responses in oxide-based lateral spin transport structures. In this paper we discuss the potential of oxide-based spin-field effect transistors and report magnetotransport data that suggest electrical spin injection into the $LaAlO_3/SrTiO_3$ interface system. In a local, three-terminal measurement scheme, we analyze the voltage variation associated with the precession of the injected spin accumulation driven by perpendicular or longitudinal magnetic fields (Hanle and 'inverted' Hanle effect). The spin accumulation signal appears to be much larger than expected, probably due to amplification effects by resonant tunneling through localized states in the $LaAlO_3$. We give perspectives on how to achieve direct spin injection with increased detection efficiency, as well on the implementation of efficient top gating schemes for spin manipulation.

Key words: oxide interfaces, spin injection.

1. Introduction

In many oxide systems several energy scales strongly compete to determine the ground state, leading to a rich variety of phases depending on internal (*e.g.* chemical doping) or external parameters (such as magnetic and electric fields or strain) [1]. Virtually all states of matter can thus be found in the oxides family (e.g. superconductivity, ferromagnetism, ferroelectricity, etc), and these states are often highly tunable. This offers immense possibilities for electronic devices, combining for instance a conductive or superconductive oxide as the channel with ferroelectrics in heteroepitaxial ferroelectric field effect transistors (FET) [2]. Magnetic oxides are no less remarkable as they include various half-metallic phases (such as doped manganese perovskites [3]) with which giant spintronics responses have been obtained. Examples include record tunnel magnetoresistance in $La_{2/3}Sr_{1/3}MnO_3/SrTiO_3/La_{2/3}Sr_{1/3}MnO_3$ magnetic tunnel junctions [4] or very large spin signals in lateral spin-valves combining $La_{2/3}Sr_{1/3}MnO_3$ and carbon nanotubes [5].

Proc. R. Soc. A 1–14; doi: 10.1098/rspa.00000000
September 6, 2011

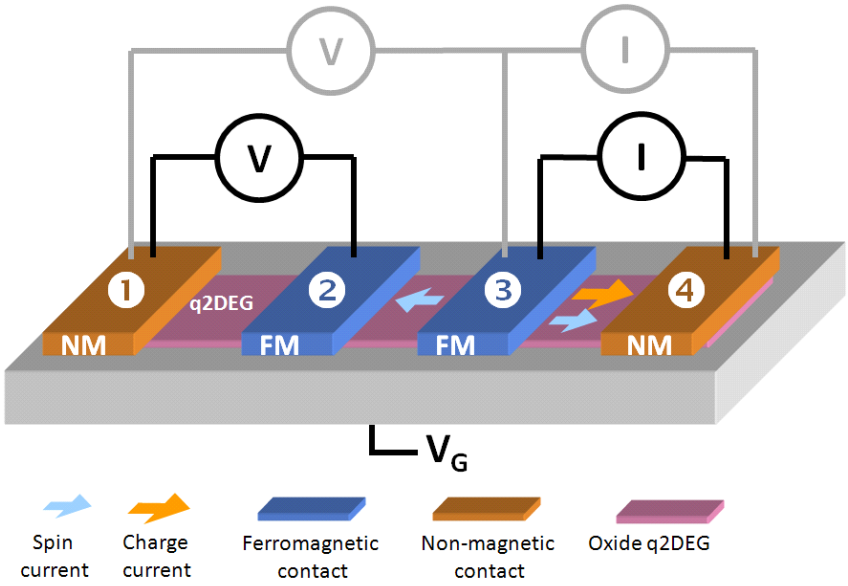

Figure 1. Sketch of a lateral spin-valve using a oxide quasi-two-dimensional electron gas (q2DEG) as the channel. The black and grey lines show 4- and 3-terminal non-local measurement geometries, respectively.

2. Motivation

In view of this outstanding ensemble of charge and spin-based phenomena and associated devices, it is tempting to try bridging the gap between gate-controlled lateral charge transport and vertical spin transport in oxide architectures. A prototypical oxide-based device for lateral spin transport is a lateral spin valve that consists of two ferromagnetic contacts (for spin injection and extraction) and an oxide q2DEG (quasi-two-dimensional electron gas) channel to transport spin information. To isolate effects due to spin transport from other magnetotransport phenomena, such as (tunnel) anisotropic magnetoresistance, it is desirable to separate spin and charge currents by resorting to non-local measurement geometries, as sketched in Fig. 1. In this device, the charge current injected between contacts 3 and 4 generates a spin current that drifts towards 4, but also diffuses towards 2. The spin-voltage V between 2 and 1 can thus be detected in a non-local fashion (*i.e.* independently of the charge voltage). Reversing the magnetization of 2 with respect to that of 3 changes the spin sensitivity and thus the sign of V. A back-gate contact enables a control of the carrier density in the oxide q2DEG and thus of the propagation of the charge and spin currents.

To probe only spin injection, and release constrains on the propagation of a spin signal from contacts 3 to 2, a three-terminal (3-T) measurement configuration (shown in grey in Fig. 1) can be used. Spin injection is then detected *via* the depolarizing effect of a perpendicular magnetic field that causes the spin-polarized

carriers to undergo Larmor precession (Hanle effect), which progressively destroys the spin accumulation as field increases [6], see 5.

In practice, to efficiently inject a spin-polarized current into a conductor, an appropriate choice of materials and architectures must be made. One of the usual difficulties resides in the conductivity mismatch between the injecting materials (typically ferromagnetic metals) and the channel materials (typically semiconductors). Several routes are possible to address this issue and achieve an efficient spin-injection. One (i) relies on the use of a ferromagnetic injector with roughly the same conductivity as the channel and another (ii) consists in inserting a tunnel barrier between the mismatched injector and channel which, in some conditions [7], may enable a good spin injection. A third, unexplored route (iii) is based on spin-filtering tunnel barriers [8, 9], in which case the injecting electrode may be a non magnetic metal. With oxides all three approaches can be pursued in epitaxial heterostructures combining materials from the same structural families, especially perosvkites. Here we have pursued route (ii) using as the tunnel barrier the 4-5 unit-cell-thick $LaAlO_3$ film used to create the q2DEG in adjacent $SrTiO_3$. The conditions for spin injection in our devices will be discussed in Section 4.

When the spin injection problem is solved, four-contact non-local spin detection in lateral spin valves may be attempted. For a finite spin signal to be detected, the dwell time of the spin-polarized electrons between the ferromagnetic injection and detection contacts must be shorter than the spin lifetime τ_{sf}. Practically, this implies than the distance between these two contacts must be shorter than the spin diffusion length and that the detection contact must be transparent enough to facilitate the extraction of the spin-polarized electrons. This thus imposes strict conditions on both the channel material and the interface between the channel and the detection contact. Although no τ_{sf} values are available for oxide-based channel materials, the recent discovery of high-mobility two-dimensional electron systems in ZnO quantum wells [10, 11], at interfaces between two insulating perovskites oxides such as $LaAlO_3$ and $SrTiO_3$ (LAO/STO) [12, 13, 14, 15] and in lightly doped STO thin films [16, 17] bring hopes of relatively long τ_{sf} values.

In the future, lateral spintronics devices based on oxide materials could eventually benefit from the outstanding multifunctional properties of transition-metal oxides and may open the way towards spin-transistors with multiple degrees of freedom, fully controllable by electric fields. As in the case of magnetic tunnel junctions, changing the magnetic configuration of the ferromagnetic contacts from parallel to antiparallel in lateral spin-valves is usually achieved by applying a magnetic field (see Fig. 2a). Taking advantage of the recent progress in artificial multiferroic tunnel junctions [18], it should be feasible to change the effective spin-polarization of the contacts by an electric field using ferroelectrics (see Fig. 2b). Inserting a ferroelectric tunnel barrier between the ferromagnetic contacts and the channel could not only result in the depletion/accumulation of charge carriers in the channel close to the ferroelectric but also change the injected spin-polarization [19]. Both phenomena will enable a non-volatile electric-field control of spin-injection in the device.

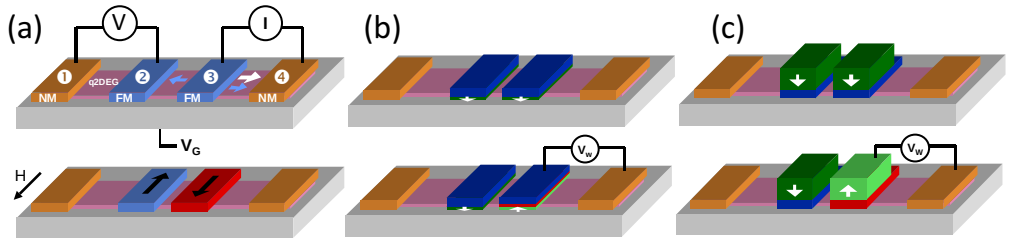

Figure 2. Lateral spin-valves in which the spin-polarization of the injected current is switched by (a) a magnetic field, (b) the ferroelectric modification of the interfacial spin-polarization, (c) the magnetoelectric modification of the contacts magnetization *via* the application of a write voltage V_w. Ferroelectric layers are shown in green.

Another possibility to control the spin-polarization of the ferromagnetic contacts without modifying the electrical conditions for spin injection and detection could consist in exploiting the magnetoelectric effect between the ferromagnetic contacts and a multiferroic [20, 21] or piezoelectric [22] grown on top, in order to control the orientation of the ferromagnets' magnetization (and as a result the effective spin-polarization), see Fig. 2c. In addition, oxides can also provide advanced gating schemes using ferroelectrics, ferromagnetic insulators or multiferroics to manipulate spin information between the injection and detection contacts. In view of this world of possibilites it is clear that besides their strong interest for electronics [23, 24], oxide q2DEGs are exciting for the exploration of novel spintronics phenomena in multifunctional heterostructures.

In this paper, we describe the fabrication of spin injection devices based on a LAO/STO q2DEG and report magnetotransport data that suggest electrical spin injection into the LAO/STO interface. Because the spin diffusion length of this system is unknown, we resort to a three-terminal measurement geometry with only one ferromagnetic tunnel contact and focus on spin injection [25], essential for future lateral spin-valves based on this system. This 3-T geometry has recently been employed to probe the spin injection efficiency in semiconductor channels [6, 26, 27, 28, 29, 30, 31, 32]. Spin injection is then detected through a correlated change of the spin splitting and voltage at the interface between the tunnel contact and the channel. Here, through combined 3-T Hanle measurements in both Voigt ($H_\perp$) and Faraday ($H_\parallel$) geometries, we present evidence of electrical spin injection into oxide-based FM/$LaAlO_3$/$SrTiO_3$ junctions, where FM is a $3d$ ferromagnet like Co.

3. Sample preparation

Films of LAO 4 to 5 unit cells thick were deposited by pulsed laser deposition on a TiO_2-terminated STO substrate, heated between 650°C and 750°C, in an oxygen pressure of 10^{-4} mbar. The KrF excimer laser (248 nm) is incident on the LAO single-crystal target with a fluence of 0.6 to 1.2 J/cm^2 at 1 Hz frequency, leading to a deposition rate of about 1 unit cell per minute on the substrate. The substrate-target distance is 77 mm. After deposition, the oxygen pressure

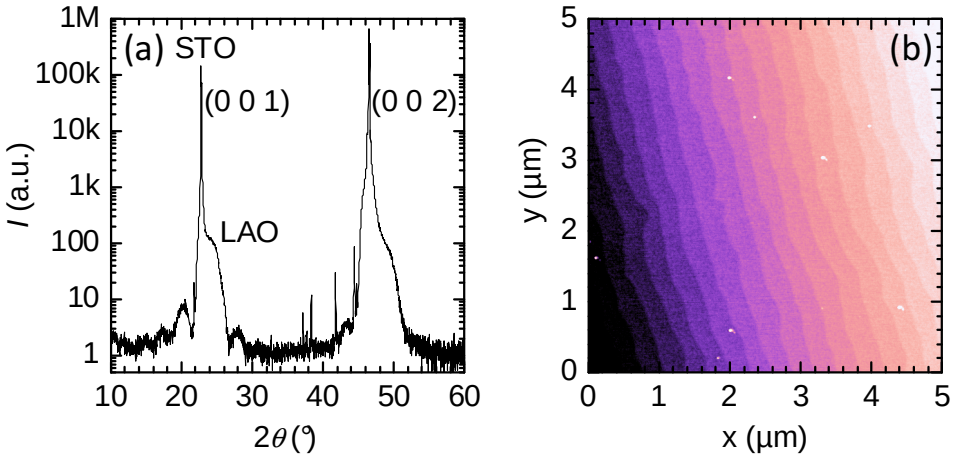

Figure 3. (a) Standard $2\theta - \omega$ diffractogram of a 9 unit-cell LAO film. Finite size (Laue) fringes are observed. The sharp extra peaks are due to absence of monochromator to filter spurious radiations lines in addition to Cu K_α (b) Atomic force microscopy (AFM) image of a 4 unit-cell sample. The color scale (height) range is 7 nm, the step height is one unit cell.

in the deposition chamber is increased to about 0.7 bar, and the temperature lowered to 500 to 550°C and kept in these conditions for 60 minutes in order to reoxygenate the STO substrate and avoid oxygen vacancies [33]. Eventually, the sample is cooled down to room temperature in one hour. Fig. 3a shows an X-ray diffraction $2\theta - \omega$ scan of a 9 unit-cell-thick LAO film that clearly displays Laue fringes adjacent to the main (001) and (002) diffraction peaks, attesting of the high structural coherence of the LAO. The obtained films are atomically flat, with the characteristic step-and-terrace morphology (Fig. 3b), each step being one-unit-cell high.

Prior to epitaxial LAO deposition, the substrate was patterned by a UV photoresist mask used to lift-off an amorphous LAO layer deposited at room temperature, a technique inspired by Ref. [34]. These amorphous areas remained insulating after the deposition of the film at high temperature, allowing us to pattern a well-defined channel. Photolithography and lift-off were also used to produce the FM electrodes, which were deposited by dc magnetron sputtering at room temperature. For the cobalt FM electrodes, a 15 or 50 nm gold layer was deposited *in situ* on top to avoid the oxidation of the thin FM layers which were 15 nm thick. Fig. 4a shows an AFM image of the device near the interface between the channel and the Co/Au contacts. The Co-based electrode film was kept thin enough in order to maintain as much as possible its magnetization in-plane, allowing observation of the Hanle effect before the reorientation of the electrode at larger magnetic field.

Aluminum wire ultrasound welding was used to contact the FM electrodes and the channel ensuring ohmic contacts with the q2DEG at the LAO/STO interface as well as with the FM electrodes, see sketch in Fig. 4b. The typical size of the tunneling contacts patterned by UV lithography for $I - V$ and Hanle measurements was 100 μm $\times$ 300 μm. Fig. 4c and d show optical images of the

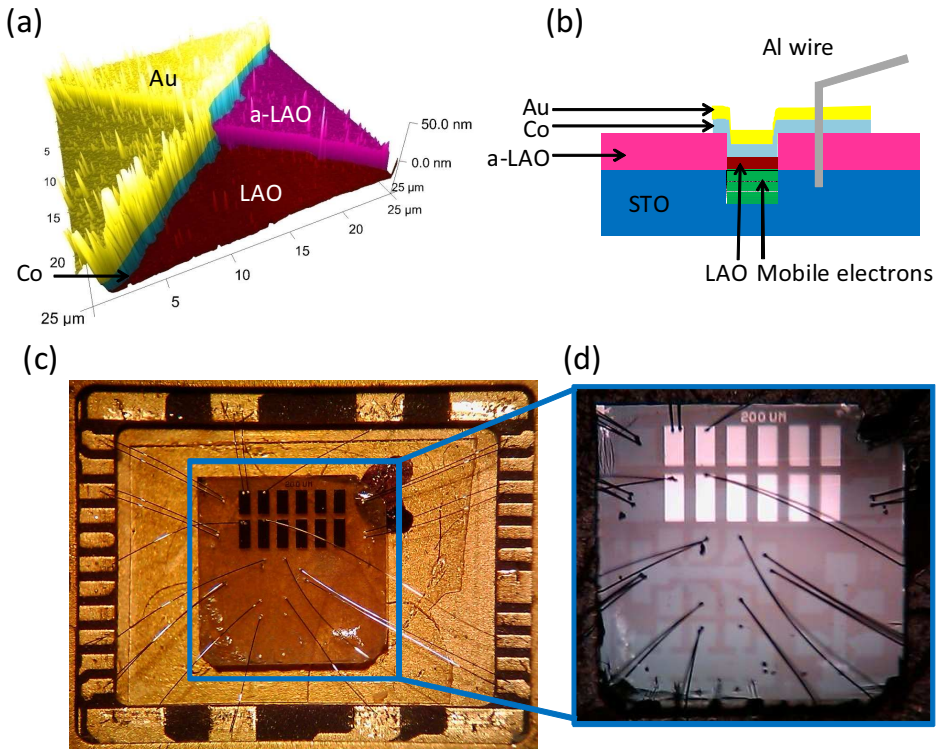

Figure 4. (a) False colour AFM image of the device after channel and top electrode definition. (b) Sketch of the device in cross-section. (c-d) Optical photographs of the device after wire bonding. Below the spin injection device (top part) Hall bars are also visible.

final device after wire bonding into the chip carrier. The resistances were mainly measured using a current source (Keithley 6220 or 6221) and a nanovoltmeter (Keithley 2182A). Field effect was applied with a voltage source which allowed the leakage current to be monitored (Keithley 2400).

4. Conditions for spin injection

As discussed by several authors including Fert *et al* [25], the efficient spin injection from a ferromagnetic metal into a semiconducting channel requires the introduction of a finite spin-conserving resistance at the interface between the ferromagnet and the channel. Practically, tunnel contacts can prove efficient for this purpose as direct tunneling is a spin-conserving process. Quantitatively and in the case of spin injection from a Co electrode into a LAO/STO q2DEG the spin-polarization of the injected current can be expressed as

$$P_{int} = \frac{\beta r_{Co} + \gamma r_b^\star}{r_{Co} + r_{2-D} + r_b^\star} \tag{4.1}$$

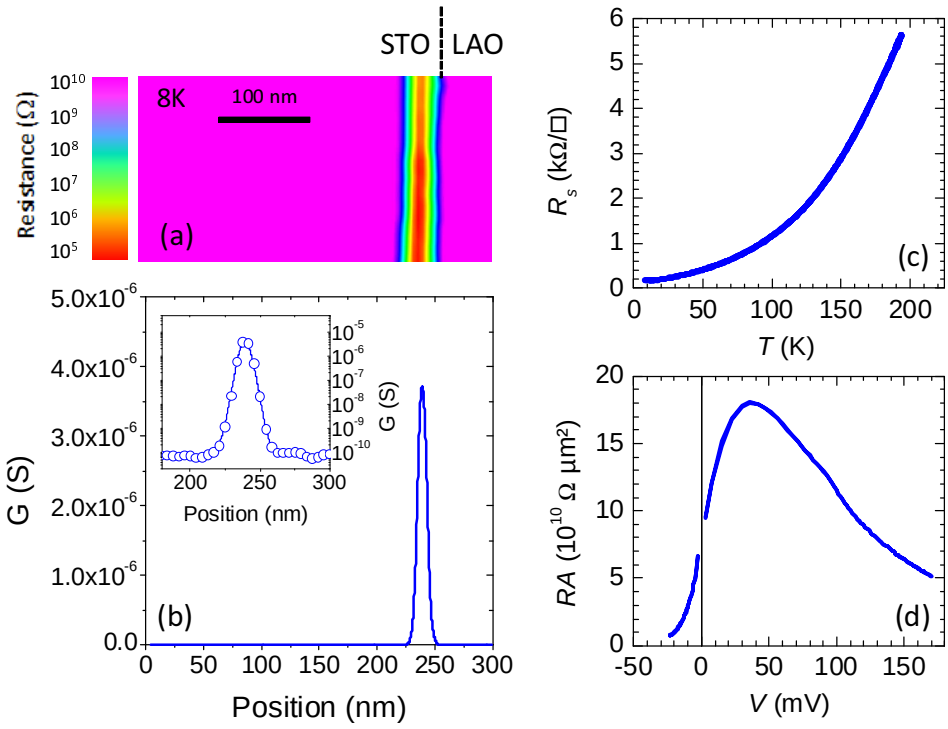

Figure 5. (a) Cross-sectional CTAFM resistance mapping of a 5 unit-cell LAO film on STO at 8K. (b) Resistance profile across the LAO/STO interface extracted from (a). Adapted from [35]. (c) Temperature dependence of the sheet resistance of the LAO/STO channel in the device. (d) Bias dependence of the resistance-area product between the Co injection contact and an ohmic Al contact on the LAO/STO channel at 12K for a 100×300 μm^2 junction.

with β and γ the spin polarization in Co and at the LAO/Co interface, respectively, r_{Co} and $r_{2-D} = R_S l_{sf}^2$ the (unit-area) spin resistance of the Co electrode and of the q2DEG (with R_S the channel sheet resistance and l_{sf} the spin diffusion length) and $r_b^\star$ the interface resistance area product.

Practically, $r_b^\star$ is likely to be much larger than r_{Co} so that the numerator of Eq.(4.1) can be approximated by $\gamma r_b^\star$. For the LAO/Co interface γ was measured by Garcia *et al* in LSMO/LAO/Co magnetic tunnel junctions showing negative tunnel magnetoresistance of about -20 % at low temperature [36]. Using Jullière's formula [37] and a spin polarization of +90 % for LSMO [38], one estimates γ=-0.1. r_{2-D} can be estimated from the sheet resistance that we plot in Fig. 5c as a function of temperature and the thickness of the q2DEG. Assuming a spin diffusion length $l_{sf} = 1$ μm and taking the value of R_S=200 Ω at 12K yields r_{2-D}=200 Ωμm^2. Importantly the thickness of the q2DEG is here much lower than l_{sf}, thereby preventing spin depolarization normal to the q2DEG plane. The q2DEG thickness was measured directly by conductive-tip AFM at low temperature in cross-section samples, as reported by Basletic *et al* [13] and Copie *et al* [35] and presented in Fig. 5a and b. From the CTAFM image it can

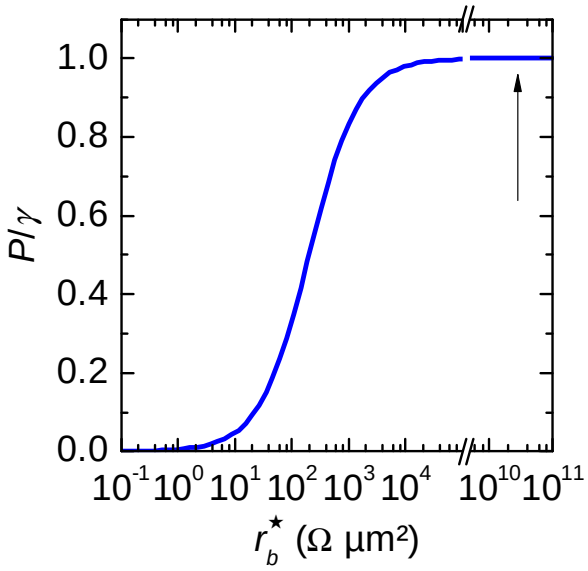

Figure 6. Dependence of the relative injected spin-polarization as a function of the interface resistance.

be appreciated that the q2DEG is confined over a finite thickness close to the LAO/STO interface. The full width at half maximum of the resistance profile (Fig. 5b) indicates a thickness of 12 nm.

Using the above parameters we can plot the injected spin polarization as function of the interface resistance $r_b^\star$, see Fig. 6. Values in excess of 10^4 $\Omega\mu$m^2 are required to achieve optimal efficiency. Experimentally the interface resistance is much larger than this threshold value, as visible from Fig. 5d that plots the resistance between the Co injection contact and an ohmic Al contact on the LAO/STO channel as a function of measurement voltage. The arrow in Fig. 6 indicates this experimental value. From this analysis we conclude that in a direct tunneling spin injection regime, an optimally spin-polarized current should be injected from Co into the LAO/STO q2DEG.

5. Magnetotransport measurements

Insight into the transport mechanism at play in the device is already provided by the typical tunneling resistance *vs.* bias curve shown in Fig. 5d, showing a clear asymmetry between positive and negative bias, reminiscent of previous observation for Au and Pt reference electrodes in Ref. [39]. This asymmetry mainly originates from the strong trapezoidal shape of the LAO barrier caused by the difference of the materials' workfunctions. The bias electric field needed to achieve measurable currents likely influences the q2DEG carrier concentration by field effect [41, 24], which considerably complicates the analysis of the corresponding $I-V$ curves that we thus do not attempt to fit.

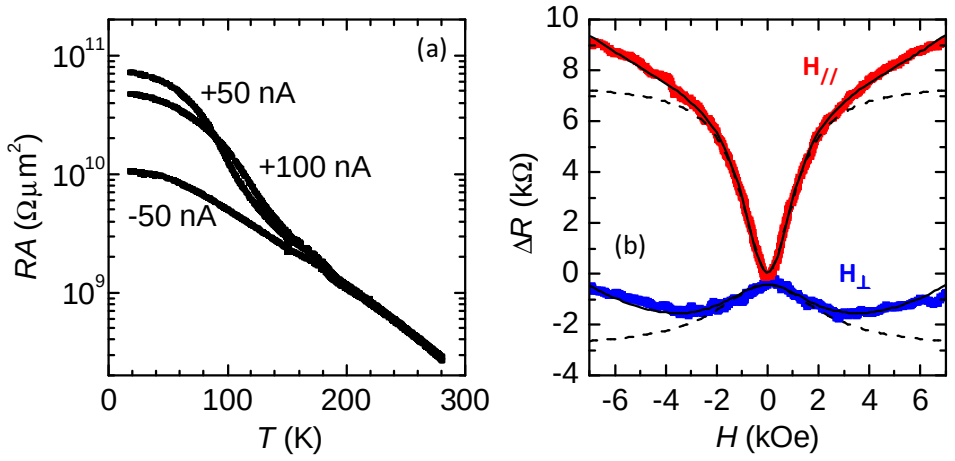

Figure 7. (a) Temperature dependence of the RA product measured at injected currents of $I = +100$, $+50$ and -50 nA. (b) Magnetoresistance as a function of magnetic field with the field applied perpendicular (Hanle effect) and parallel (inverse Hanle effect) to the sample plane, at 2K. The solid lines are fits with a lorentzian plus a parabolic background and the dashed lines show only the lorentzian contribution due to the Hanle effect. Adapted from Reyren *et al* [40].

In contrast to the channel sheet resistance that *decreases* with temperature (Fig. 5c) we have found that the resistance $Co/LaAlO_3/SrTiO_3$ junctions strongly *increases* with temperature, in a thermally activated way, see Fig. 7a. Data acquired at positive current (electrons injected from the q2DEG towards the FM electrode) display a very strong temperature dependence and the RA product increases by almost three orders of magnitude from 300 K to 10 K. This is a clear signature of inelastic tunneling transport processes through localized states (LS) embedded in the LAO barrier. We infer that these LS are partitioned in LAO at the LAO/STO interface with characteristic occupation energy levels close to the Fermi level of the q2DEG in STO. Owing to the band structure articulation at LAO/STO interfaces highlighted by *in situ* photoemission [42] and to the position of the electronic level of intrinsic defects in LAO calculated by density-functional theory (DFT) [43, 44], such LS are likely played by oxygen vacancies or intermixing [45, 46] in LAO. This leads to available electronic states accessible for spin injection at $3s-3p$ Al or $6s-5d$ La on-site orbitals. Other different point defects in LAO, like ionized interstitial Al^{3+} or La^{3+}, are also possible candidates [43]. This is discussed further later.

We now turn on to Hanle magnetoresistance (MR) data. Fig. 7b shows typical 3-T Hanle signal, acquired at 2 K and at positive current $I = +50\ nA$ (+0.13 V bias), in standard Voigt geometry (field perpendicular to the plane $H_\perp$) and Faraday geometry (field in the plane $H_\parallel$) [40]. Aside from a superimposed parabolic background, the $H_\perp$ curve displays a quasi Lorentzian shape of about 2 kΩ (60 MΩ · μm^2 of resistance-area) amplitude compared to the base 2.7 MΩ (80 GΩ · μm^2, see Fig. 5d) resistance, that is a total MR of 0.7%. This negative MR evidences a correlated drop of the spin splitting $\Delta\mu = \mu_\uparrow - \mu_\downarrow$ (with $\mu_{\uparrow,\downarrow}$ the respective electrochemical potential for spin $\uparrow, \downarrow$) and voltage ΔV according to

$\Delta V = \gamma \Delta\mu/(2e)$, [47, 48] where e is the electronic charge. A primary analysis leads to a splitting of the chemical potential $\Delta\mu(H)$ of the form $\Delta\mu(0)/\left[1+(\omega_L\tau_{sf})^2\right]$, where ω_L is the Larmor frequency, and a characteristic spin-relaxation time τ_{sf} can be extracted from the width of the Lorentzian. Correspondingly, the MR curves (Fig. 7b) are fitted by $R(H) = R(0)/\left[1+(\omega_L\tau_{sf})^2\right]$ plus a parabolic background, where $\omega_L = g_e\mu_B H/\hbar$ is calculated by assuming a Landé factor g_e=2. Using such a procedure, we would extract a typical value of $\tau_{sf} = 50$ ps at 2 K. Considering a diffusion constant $\mathcal{D} \simeq 40$ cm^2 s^{-1} [49] this corresponds to a spin-diffusion length $\ell_{sf} = \sqrt{\mathcal{D}\tau_{sf}} \approx 1\,\mu$m. Nevertheless, alternative mechanisms of spin depolarization caused by random magnetic fields may modify the Hanle signals as well as artificially enlarge the width of the Lorentzian shape [30].

In order to go beyond this first simple analysis, Fig. 7b also presents the results of Hanle experiments in a Faraday geometry where the magnetic field was applied along the direction of the injected spins. In the field scale limit of ~ 0.7 T a total Hanle (normal + inverted) signal ΔR_H of about 10 kΩ (0.3 G$\Omega \cdot \mu$m^2) is measured before reorientation of the Co magnetization occurring around 1.8 T (not shown). Striking similarities with the signals obtained at FM/AlO_2/Si junctions [30] suggests that common mechanisms of spin injection occur in these systems and thus explain a *negative* peak (inverted Hanle curve) in the magnetoresistance data. This may originate from the presence of a random magnetic field causing precession and loss of spin accumulation. In other words, the application of a transverse magnetic field results in a loss of spin coherence, while an external field applied parallel to the injected spin restores the spin accumulation. It results that ΔR_H should scale with the total amplitude of spin accumulation at LAO/STO interface. However, we note that this spin signal is enhanced by more than *five orders of magnitude* compared to intrinsic spin resistance $R^s_{ch} = R_\square \times l^2_{sf}$ of the q2DEG evaluated at $\sim 100\ \Omega \cdot \mu$m^2 for a typical l_{sf} of 1 μm, indicating that some highly efficient amplification process is at play as in Tran *et al.* [26]. Further experiments on the influence of the bias and gate voltage are under way to understand better this phenomenon.

We now discuss in more detail the possible origin of the random field, among stray field [30], Rashba spin-orbit field [501, 49], and hyperfine interactions [51, 52], responsible for spin decoherence. In the present case, one can easily discard stray field effects as the LAO surface is atomically flat, with only one unit-cell steps ($\sim$ 4 Å) over 200 nm wide terraces. On the other hand, Rashba spin-orbit interactions [501, 49] are known to vanish on (non propagative) localized states. More likely, as for the case of hybrid organic spin valves [53] or ZnO oxide quantum dots [54], the random field may have an hyperfine origin, Al^{3+} and La^{3+} sites (Al or La antisites or bounded to oxygen vacancies) bearing respectively a nuclear moment of $I_{\rm Al} = 5/2$ for ^{27}Al (with a 100% abundance) and $I_{\rm La} = 7/2$ for ^{139}La (with a 99.91% abundance). In this scenario, electrons are subject to a nuclear field [55, 51]:

$$H_{\rm n} \;=\; \frac{2}{3}\mu_0 g_n \mu_B \hbar \vec{I}\cdot\vec{S}\,|\psi(0)|^2$$

where g_n is the nuclear gyromagnetic ratio ($g_n^{Al} = 1.4566$, $g_n^{La} = 0.7952$) and $\psi(0)$ is the weight of their respective $3s$- and $6s$-type wavefunction at the center. Taking into account the respective value for g_n, a good estimate of the nuclear field for

both Al and La is about $0.1 - 0.2$ T taking into account the typical extension of their wavefunction. [56] In an inverted Hanle experiment (Faraday geometry), and in the limit of a long spin-lifetime the voltage drop ΔV measured at a junction equals [30] $\Delta V = \frac{\gamma}{2}\Delta\mu/e\left\langle\cos^2(\theta)\right\rangle$ where θ is the angle between the spin and the effective magnetic field, sum of the random nuclear fields, H_n, and the external field H. The resistance variation $\Delta R_H \propto \left\langle\cos^2(\theta_H)\right\rangle$ slightly departs from a standard Lorentzian shape according to the formula (see Fig.):

$$\Delta R_H(H_{||}) \propto \frac{3}{4} - \frac{1}{4h^2} + \frac{(1-h^2)^2}{8h^3}\ln\left|\frac{1+h}{1-h}\right| \tag{5.1}$$

where h is the reduced field $H_{||}/H_n$. The total amplitude of the inverted Hanle effect is then $2/3$ of the total amplitude of $\Delta R_H = \frac{\gamma\Delta\mu}{2j}$. This corresponds to a gradual restoration of the spin accumulation in proportion $2/3$, while the normal Hanle effect has a proportion of $1/3$ as one can expect. Then, the particular value of the external field $H_{1/4}$, corresponding to $h = 1$ and for which $\Delta R_H(H_{1/4}) = \frac{3}{4}\Delta R_H(0) + \frac{1}{4}\Delta R_H(H_\infty)$, gives the magnitude of the random field that lies around 0.1 T in agreement with the estimation of the nuclear field of Al and La given above.

6. Conclusion

In conclusion, we have investigated spin injection from a magnetic tunnel contact towards the $LaAlO_3/SrTiO_3$ two-dimensional electron system by using a three-terminal Hanle approach in both Voigt and Faraday geometries. Both the Hanle and inverted Hanle signals are strongly enhanced, consistant with amplification effects by localized states positioned in the $LaAlO_3$ barrier midgap, possibly associated with oxygen vacancies or intermixing. We propose that the inverted Hanle effect is due to spin depolarization by random nuclear fields. In order to detect the direct injection of spin-polarized carriers into the $LaAlO_3/SrTiO_3$ channel, either the injection contact resistance must be significantly reduced, for instance by replacing $LaAlO_3$ with a lower gap material, or four-contact non-local detection schemes must be implemented. This would require distances between injector and detector smaller than the characteristic spin-diffusion length, which should be achievable with electron-beam lithography techniques. Resorting to lightly doped $SrTiO_3$ films with higher electron mobilities may be another way to reduce the constraints on channel dimensions.

Acknowledgment

We thank E. Jacquet and R. Bernard for technical help with the PLD setup. We acknowledge financial support from the French Agence Nationale de la Recherche (project "Oxitronics") and the Triangle de la Physique (project "Easox").

References

1 E. Dagotto, Complexity in strongly correlated electronic systems, *Science* **309** (2005), 257–262.

2 C.H. Ahn, A. Bhattacharya, M. Di Ventra, J.N. Eckstein, C.D. Frisbie, M.E. Gershenson, A.M. Goldman, I.H. Inoue, J. Mannhart, A.J. Millis, A.F. Morpurgo, D. Natelson and J.-M. Triscone, Electrostatic modification of novel materials, *Rev. Mod. Phys.* **78** (2006), 1185–1212.

3 J.M.D. Coey, M. Viret, and S. von Molnàr, Mixed-valence manganites, *Adv. Phys.* **58** (1999), 167–293.

4 M. Bowen, M. Bibes, A. Barthélémy, J.P. Contour, A. Anane, Y. Lemaître, and A. Fert, Nearly total spin polarization in $La_{2/3}Sr_{1/3}MnO_3$ from tunneling experiments, *Appl. Phys. Lett.* **82** (2003), 233–235.

5 L. E. Hueso, J.M. Pruneda, V. Ferrari, G. Burnell, J.P. Valdes-Herrera, B.D. Simons, P.B. Littlewood, E. Artacho, A. Fert, and N.D. Mathur, Transformation of spin information into large electrical signals using carbon nanotubes, *Nature* **445** (2007), 410–413.

6 X. Lou, C. Adelmann, M. Furis, S.A. Crooker, C.J. Palmstrøm, and P.A. Crowell, Electrical Detection of Spin Accumulation at a Ferromagnet-Semiconductor Interface, *Phys. Rev. Lett.* **96** (2006), 176603.

7 A. Fert and H. Jaffrès, Conditions for efficient spin injection from a ferromagnetic metal into a semiconductor, *Phys. Rev. B* **53** (2002), 323.

8 M. Gajek, M. Bibes, A. Barthélémy, K. Bouzehouane, S. Fusil, M. Varela, J. Fontcuberta, and A. Fert, Spin filtering through ferromagnetic $BiMnO_3$ tunnel barriers, *Phys. Rev. B* **72** (2005), p. 020406.

9 U. Luders, M. Bibes, K. Bouzehouane, E. Jacquet, J.P. Contour, S. Fusil, J.F. Bobo, J. Fontcuberta, A. Barthélémy, and A. Fert, Spin filtering through ferrimagnetic $NiFe_2O_4$ tunnel barriers, *Appl. Phys. Lett.* **88** (2006), 082505.

10 S. Ghosh, V. Sih, W.H. Lau, D.D. Awschalom, S.-Y. Bae, S. Wang, S. Vaidya, and G. Chapline, Room-temperature spin coherence in ZnO, *Appl. Phys. Lett.* **86** (2005), 232507.

11 A. Tsukazaki, S. Akasaka, K. Nakahara, Y. Ohno, H. Ohno, D. Maryenko, A. Ohtomo, and M. Kawasaki, Observation of the fractional quantum Hall effect in an oxide, *Nature Mater.* **9** (2010), 889-893.

12 A. Ohtomo and H.Y. Hwang, A high-mobility electron gas at the $LaAlO_3/SrTiO_3$ heterointerface, *Nature* **427** (2004), 423–426.

13 M. Basletic, J.L. Maurice, C. Carrétéro, G. Herranz, O. Copie, E. Jacquet, K. Bouzehouane, S. Fusil, and A. Barthélémy, Mapping the spatial distribution of charge carriers in $LaAlO_3/SrTiO_3$ heterostructures, *Nature Mater.* **7** (2008), pp. 621–625.

14 A. D. Caviglia, S. Gariglio, C. Cancellieri, B. Sacépé, A. Fête, N. Reyren, M. Gabay, A. F. Morpurgo, and J.-M. Triscone, Two-dimensional quantum oscillations of the conductance at $LaAlO_3/SrTiO_3$ interfaces, *Phys. Rev. Lett.* **105** (2010), 236802.

15 M. Ben Shalom, A. Ron, A. Palevski, and Y. Dagan, Shubnikov-de Haas oscillations in $SrTiO_3/LaAlO_3$ interface, *Phys. Rev. Lett.* **105** (2010), 206401.

16 Y. Kozuka, M. Kim, C. Bell, B.G. Kim, Y. Hikita, and H.Y. Hwang, Two-dimensional normal-state quantum oscillations in a superconducting heterostructure, *Nature* **462** (2009), 487–490.

17 J. Son, P. Moetakef, B. Jalan, O. Bierwagen, N.J. Wright, R. Engel-Herbert, and S. Stemmer, Epitaxial $SrTiO_3$ films with electron mobilities exceeding 30,000 $cm^2V^{-1}s^{-1}$, *Nature Mater.* **9** (2010), 482.

18 V. Garcia *et al.*, Ferroelectric control of spin polarization, *Science* **327** (2010), 1106–1110.

19 M.Y. Zhuravlev, S.S. Jaswal, E.Y. Tsymbal, and R.F. Sabirianov, Ferroelectric switch for spin injection, *Appl. Phys. Lett.* **87** (2005), 222114.

20 M. Bibes and A. Barthélémy, Towards a magnetoelectric memory, *Nature. Mater.* **7** (2008), 425–426.

21 S. M. Wu, S.A. Cybart, P. Yu, M. D. Rossell, J. X. Zhang, R. Ramesh, and R. C. Dynes, Reversible electric control of exchange bias in a multiferroic field-effect device, *Nature Mater.* **9** (2010), 756–761.

22 M. Weiler *et al.*, Voltage controlled inversion of magnetic anisotropy in a ferromagnetic thin film at room temperature, *New J. Phys.* **11** (2009), 013021.

23 C. Cen, S. Thiel, J. Mannhart, and J. Levy, Oxide nanoelectronics on demand, *Science* **323** (2009), 1026–1030.

24 R. Jany *et al.*, Diodes with breakdown voltages enhanced by the metal-insulator transition of $LaAlO_3$-$SrTiO_3$ interfaces., *Appl. Phys. Lett.* **96** (2010), 183504.

25 A. Fert, J.-M. George, H. Jaffrès, and R. Mattana, Semiconductors between spin-polarized sources and drains., *IEEE Trans. Electron Dev.* **54** (2007), 921.

26 M. Tran, H. Jaffrès, C. Deranlot, J.-M. George, A. Fert, A. Miard, and A. Lemaître, Enhancement of the spin-accumulation at the interface between a spin-polarized tunnel junction and a semiconductor, *Phys. Rev. Lett.* **102** (2009), p. 036601.

27 S.P. Dash, S. Sharma, R.S. Patel, M.P. de Jong, and R. Jansen, Electrical creation of spin polarization in silicon at room temperature., *Nature* **462** (2009), p. 491.

28 T. Sazaki, T. Oikawa, T. Suzuki, M. Shiraishi, Y. Suzuki and K.Noguchi, Comparison of spin signals in silicon between nonlocal four-terminal and three-terminal methods., *Appl. Phys. Lett.* **96** (2010), 122101.

29 T. Suzuki, T. Sazaki, T. Oikawa, M. Shiraishi, Y. Suzuki and K. Noguchi, Room-temperature electron spin transport in a highly doped Si channel., *Appl. Phys. Express* **4** (2011), 023003.

30 S.P. Dash, S. Sharma, J.C. Le Breton, J. Peiro, H. Jaffrès, J.-M. George, A. Lemaître, and R. Jansen, Spin precession and decoherence near an interface with a ferromagnet., *Phys. Rev. B* **84** (2011), 054410.

31 C.H. Li, O.M.J. van't Erve, and B.T. Jonker, Electrical injection and detection of spin accumulation in silicon at 500 K with magnetic metal/silicon dioxide contacts., *Nature Comm.* **2** (2011), 245.

32 Y. Ando *et al*, Bias current dependence of spin accumulation signals in a silicon channel detected by a Schottky tunnel contact, (2011), arXiv.org:1104.2658v1.

33 C. Cancellieri *et al*, Influence of the growth conditions on the $LaAlO_3/SrTiO_3$ interface electronic properties., *Europhys. Lett.* **91** (2010), 17004.

34 C.W. Schneider, S. Thiel, G. Hammerl, C. Richter, and J. Mannhart, Microlithography of electron gases formed at interfaces in oxide heterostructures., *Appl. Phys. Lett.* **89** (2006), 122101.

35 O. Copie *et al*, Towards Two-Dimensional Metallic Behavior at $LaAlO_3/SrTiO_3$ Interfaces, *Phys. Rev. Lett.* **102** (2009), 216804.

36 V. Garcia, M. Bibes, J.L. Maurice, E. Jacquet, K. Bouzehouane, J.P. Contour, and A. Barthélémy, Spin-dependent tunneling through high-k $LaAlO_3$, *Appl. Phys. Lett.* **87** (2005), 212501, 212501.

37 M. Julliere, Tunneling between ferromagnetic films, *Phys. Lett. A* **54** (1975), 225–226.

38 V. Garcia, M. Bibes, A. Barthélémy, M. Bowen, E. Jacquet, J.P. Contour, and A. Fert, Temperature dependence of the interfacial spin polarization of $La_{2/3}Sr_{1/3}MnO_3$, *Phys. Rev. B* **69** (2004), 052403.

39 G. Singh-Bhalla, C. Bell, J. Ravichandran, W. Siemons, Y. Hikita, S. Salahuddin, A.F. Hebard, H.Y. Hwang, and R. Ramesh, Built-in and induced polarization across $LaAlO_3/SrTiO_3$ heterojunctions., *Nature Phys.* **7** (2011), 80.

40 N. Reyren, M. Bibes, E. Lesne, J.-M. George, C. Deranlot, S. Collin, A. Barthélémy and H. Jaffrès, *submitted to Phys. Rev. Lett.*

41 S. Thiel, G. Hammerl, A. Schmehl, C.W. Schneider, and J. Mannhart, Tunable Quasi-Two-Dimensional Electron Gases in Oxide Heterostructures, *Science* **313** (2006), 1942–1945.

42 K. Yoshimatsu, R. Yasuhara, H. Kumigashira, and M. Oshima, Origin of metallic states at the heterointerface between the band insulators $LaAlO_3$ and $SrTiO_3$., *Phys. Rev. Lett.* **101** (2008), 026801.

43 X. Luo, B. Wang, and Y. Zheng, First-principles study on energetics of intrinsic point defects in $LaAlO_3$., *Phys. Rev. B* **80** (2009), 104115.
44 Z. Zhong, P.X. Xu, and P. Kelly, Polarity-induced oxygen vacancies at $LaAlO_3/SrTiO_3$ interfaces., *Phys. Rev. B* **82** (2010), 165127.
45 N. Nakagawa, H.Y. Hwang, and D.A. Muller, Why some interfaces cannot be sharp, *Nature Mater.* **5** (2006), 204–209.
46 S.A. Pauli and others, Evolution of the Interfacial Structure of $LaAlO_3$ on $SrTiO_3$., *Phys. Rev. Lett.* **106** (2011), 036101.
47 A. Brattas, G.E.W. Bauer, and P.J. Kelly, Non-collinear magnetoelectronics., *Phys. Rep.* **427** (2006), 157–256.
48 J. Barnás, A. Fert, M. Gmitra, I. Weymann, and V.K. Dugaev, From giant magnetoresistance to current-induced switching by spin transfer., *Phys. Rev. B* **72** (2005), 024426.
49 A. D. Caviglia, M. Gabay, S. Gariglio, N. Reyren, C. Cancellieri, and J.-M. Triscone, Tunable Rashba spin-orbit interaction at oxide interfaces., *Phys. Rev. Lett.* **104** (2010), 126803.
50 M. Ben Shalom, M. Sachs, M. Rakhmilevitch, A. Palevski, and Y. Dagan, Tuning spin-orbit coupling and superconductivity at the $SrTiO_3/LaAlO_3$ interface: a magnetotransport study., *Phys. Rev. Lett.* **104** (2010), 126802.
51 D. Paget, G. Lampel, B. Sapoval, and V.I. Safarov, Low field electron-nuclear spin coupling in gallium arsenide under optical pumping conditions., *Phys. Rev. B* **15** (1977), 5780.
52 I.A. Merkulov, A.L. Efros, and M. Rosen, Electron spin relaxation by nuclei in semiconductor quantum dots., *Phys. Rev. B* **65** (2002), 205309.
53 J.J.H.M. Schoonus, P.G.E. Lumens, W. Wagemans, J.T. Kohlhepp, P.A. Bobbert, H.J.M. Swagten and B. Koopmans, Magnetoresistance in hybrid organic spin valves at the onset of multiple-step tunneling., *Phys. Rev. Lett.* **103** (2009), p. 146601.
54 W.K. Liu *et al.* Room-temperature electron spin dynamics in free-standing ZnO quantum dots. *Phys. Rev. Lett.* **98,** 186804 (2007).
55 S. Millman and P. Kush, Nuclear spin and magnetic moment of $^{27}_{13}$Al., *Phys. Rev.* **56** (1939), 303.
56 R.D. Cowan *The theory of atomic structure and spectra* Ch. 7-8 (University of California Press, Berkeley, Los Angeles, London, 1981).